Differences in Gut Microbiota Assembly Alter Its Ability to Metabolize Dietary Polysaccharides and Resist *Clostridioides difficile* Colonization

Matthew K. Schnizlein[a], Alexandra K. Standke[b], Mark J. Garmo[a], Summer J. Edwards[b], Vincent B. Young[a,b,#]

[a]Department of Microbiology and Immunology, University of Michigan, Ann Arbor, MI, USA
[b]Department of Internal Medicine, University of Michigan, Ann Arbor, MI, USA

Corresponding author: Vincent B. Young, youngvi@umich.edu

Abstract: The mammalian gut is home to a vibrant community of microbes. As the gut microbiota has evolved, its members have formed a complex yet stable relationships that prevent non-indigenous microorganisms, such as *Clostridioides difficile*, from establishing within the gut. Using a bioreactor model of the gut, we characterize how variation in microbial community assembly changes its ability to resist *C. difficile*. We established diluted microbial communities from healthy human stool in a bioreactor gut model and subsequently challenged them with vegetative *C. difficile*. 16S rRNA-gene sequencing and selective plating revealed that dilution progressively increases microbiota variability and decreases C*. difficile* colonization resistance. Using Dirichlet Multinomial Mixtures and linear discriminant analysis of effect size, we identified 19 bacterial taxa, including *Bifidobacterium, Bacteroides* and Lachnospiraceae, that associate with more resistant community types. Since these taxa are associated with butyrate production, which is tied to *C. difficile* colonization resistance, we performed another reactor experiment where we increased inulin concentrations prior to *C. difficile* challenge. Diluted communities concurrently lost their ability to produce additional butyrate in response to inulin, as

measured by high performance liquid chromatography, and resist *C. difficile* colonization. These data demonstrate that a similar level of microbiota cohesiveness is required to prevent *C. difficile* colonization and metabolize inulin. It also suggests that metabolic activity of butyrate-producing microbes is tied to colonization resistance. Future work can leverage these findings to develop treatments that leverage knowledge of these ecological dynamics to improve efficacy.

Importance: The microbes living in the human large intestine helps create an environment that is resistant to organisms that do not normally reside there, such as the pathogen *Clostridioides difficile*. Differences in ways in which microbial communities make an environment their home can change their ability to provide that resistance. To study those differences, we use a model of the intestine that incorporates only microbial variables (i.e. no host is involved). By diluting microbial communities to decrease their complexity, we show that communities lose their ability to resist *C. difficile* at a particular point and, at the same time, their ability to use inulin, a common dietary fiber, in ways that make the environment more toxic to *C. difficile*. These findings will help future researchers dissect the microbial components that create a resistant intestinal environment.

1. Introduction

The mammalian gut contains a complex ecosystem with a variety of fungal, bacterial, archaeal and viral organisms that exist in a network of metabolic interactions. These vast arrays of interactions regulate microbial competition and impact the host. External stability, otherwise known as colonization resistance, is a complex phenomenon in which resident taxa prevent the invasion of foreign ones by occupying niches in an environment. For example, probiotic organisms fail to exist long-term in the gut because resident microbes are better able to compete for niche space (1). These interactions have also been observed to prevent colonization of pathogenic organisms such as *Escherichia coli*, *Salmonella* Typhimurium, and *Clostridioides difficile* (2-5).

In studying colonization resistance, several models, including humans, mice, enteroids and bioreactors, have been used to ascertain characteristics of a resistant environment (5-13). Each of these models supports a unique level of complexity that may consider host-microbe, microbe-microbe, and microbe-environment interactions. Bioreactors have been used extensively to study the microbiota of the gut environment, particularly the dynamics of microbe-mediated colonization resistance. This is due in part to the controlled way nutrients flow in and out of the system. In the context of resistance to *C. difficile*, healthy human stool established in these reactors prevents or limits colonization (14, 15). However, alterations to the resident microbiota can reduce the ecosystem's ability to do so (15-17).

Since much of colonization resistance revolves around microbial metabolism, host dietary inputs play an important role in modulating this phenotype. As previous studies have demonstrated, both macronutrients (e.g., proteins and polysaccharides) and

cofactors (e.g., vitamins and minerals) can modulate *C. difficile* colonization resistance by affecting the resident microbiota and host immune system (18-20). Much like "macroorganisms" adapt to the food available to them, microbes alter their metabolism to capitalize on the nutrient sources in their surroundings. These metabolic shifts lead to different downstream products with which other organisms in the ecosystem interact.

While previous work has characterized forced effects (e.g., antibiotic use) on microbiota post-establishment, limited work has characterized the stochastic processes of community establishment in the context of *C. difficile* colonization resistance (14, 21, 22). To manipulate the microbiota to treat infections, a fuller grasp of the ecological rules underlying community physiology is needed. Specifically, further work is required to accurately describe how random and specific effects alter community establishment and ability to resist the colonization of non-indigenous microbes. Here we describe how stochastic effects, as induced by community dilution, and directed effects, as induced by supplementation with additional carbohydrates, influence the establishment of a microbial community. We also characterize how the functional effects of this variation alter metabolic output and colonization resistance to *Clostridioides difficile.*

2. Results

2.1. Dilution of starting inoculum alters establishment dynamics of continuous flow cultures

Using a bioreactor system initially developed by Auchtung et al., we extended studies on how dilution impacts the membership and variability of microbial communities (14, 22). We established communities in bioreactors from serially diluted stool samples

taken from a healthy human donor (10^{-3}, N=4; 10^{-5}, 10^{-7}, and 10^{-9}, N=6). Following inoculation of the reactors, communities were given one day to equilibrate in static culture before initiating continuous flow. The subsequent 6 days in continuous flow allowed communities time to adjust before testing their external stability with a model invasive bacterium, *C. difficile* (Fig. 1A).

Dilution increased the variability of communities and lowered the number of taxa that became established. By day 6, 16S rRNA-gene sequencing analysis showed that 93±6 and 60±15 operational taxonomic units (OTUs) became established in those communities diluted 10^{-3} and 10^{-5}, respectively (Fig. 1B & Fig. S1A). Communities from these stool dilutions consisted mainly of Bacteroidota and Bacillota (Fig. 1D-E). Reactors established with more diluted fecal inocula had fewer OTUs established by day 6 (i.e., 10^{-7} and 10^{-9} dilutions had 45±20 and 40±23 OTUs, respectively) and also unique proportions of bacterial phyla, with some being dominated by Actinomycetota and others by Pseudomonadota (Fig. 1B & Fig. 1F-G). More diluted inocula established in individualized community structures in each reactor replicate (Fig. S1C-F).

This variability is captured by principal coordinate analysis, which shows that dilution altered the dynamics of each community's establishment so that they cluster separately (Fig. 1C). Dissimilarity between replicate reactors in each group increased as the dilution factor increased, as measured by Bray-Curtis and Jaccard Dissimilarity Indexes, which capture the abundance and the presence/absence of taxa, respectively (Fig. 2A-B). This variability trend was also observed when comparing multiple timepoints within each individual reactor (Fig. S2A-B). While dilution greatly reduced the initial biomass of microbes, after 6 days of growing in continuous culture, communities had

reached similar levels of abundance as measured by qPCR of the 16S rRNA-gene (Fig. S1B).

2.2. Dilution decreases resistance to a model invasive organism

C. difficile is a model organism that can generally not invade communities unless they have been perturbed. Since dilution increased community variability, which is a marker of external stability, we hypothesized that this would result in reduced ability to prevent *C. difficile* colonization. 7 days after establishment of bioreactor communities, they were challenged with 10^4 vegetative *C. difficile* cells. As measured by colony-forming units (CFU), communities possessed varying capabilities to resist colonization with *C. difficile* (Fig. 3A). Within 24 hrs of challenge, 3 of 4 communities diluted 10^{-3} prevented *C. difficile* colonization while communities diluted 10^{-9} showed colonization levels around 10^7 CFU/mL in all six replicates. The largest intra-group variation in colonization was observed in the 10^{-5}, where all six reactors had intermediate levels of colonization, and 10^{-7} dilutions, which had three reactors colonize at 10^7 and three fully resist. Since *C. difficile* colonizes at 10^7 CFU/mL when it grows by itself in a reactor (data not shown), our data suggest that reactor communities that reached this level had no colonization resistance. Furthermore, 24 hrs after *C. difficile* challenge, those communities experienced a loss of resident taxa (37±21 on day 6 to 14±4 on day 7; Wilcoxon Rank Sum Test, $p < 0.01$), demonstrating that these microbial communities had both no ability to resist a non-indigenous microbe or remain intact (Fig. S3A-C).

Using Dirichlet Multinomial Modelling (DMM), we identified 3 community types across the established communities, which associated with dilution (Fig. 3B). Of these,

type 3 supported significantly lower colonization than enterotypes 1 and 2, with type 1 supporting a middle level of colonization (Fig. 3C). Through LEfSe, we identified 19 taxa associated with the more resistant enterotypes (i.e., enterotypes 1 & 3; Fig. S3D) and five associated with enterotype 2 (Fig. S3E). We noted several commonly associated with metabolic functions known to increase resistance to *C. difficile*, such as short-chain fatty acid (SCFA) production. These taxa included *Bifidobacterium, Bacteroides*, *Blautia, Faecalibacterium,* Unclassified Lachnospiraceae and *Clostridium* (sensu stricto) (Fig. 3D & Fig. S3D-E).

2.3. Diluted communities respond uniquely to a change in carbohydrate concentrations

The dilution experiments above indicated that colonization resistance against *C. difficile* was associated with the presence of taxa that could degrade dietary polysaccharides and produce SCFAs (20, 23). Other work has indicated that SCFAs are able to limit the growth of *C. difficile* (20). Therefore, we characterized how a change to higher carbohydrate concentrations affected the formation of communities and their ability to resist *C. difficile* colonization following a bottleneck event. We chose to increase the availability of the carbohydrate inulin due to its ability to induce the production of SCFAs by the gut microbiota (24-26). We also opted to use this polysaccharide due to the association of microbes with inulin catabolic potential and colonization resistance in the dilution experiment. Using a second fecal donor, we established reactor communities using feces diluted 10^{-3}, 10^{-4}, 10^{-5} and 10^{-6}. Based on our work above we hypothesized that these dilutions would result in communities that might support moderate levels of *C.*

difficile colonization. After growing communities for two days on standard BRM, which contains 0.02% inulin, we increased inulin concentrations to 0.2% (Fig. 4A). Despite the narrower range of dilution, communities established in these reactors again differed in the number of OTUs that became established, with less diluted communities having a significantly higher number of resident OTUs (Fig. 4B). While we observed a shift in the Bray-Curtis distance relative to baseline in the community diluted 10^{-3} when comparing days 2 and 5, we did not observe a statistically significant change in the number of OTUs (Fig. 4B & Fig. S4A). There was no shift in ecologic distance in the other dilution groups. Despite the minimal changes in community structure, there was a significant shift in metabolic activity of these communities in terms of carbohydrate metabolism with a drop in acetate and a 3-fold increase in butyrate concentrations (Fig. 4C). There was no change in propionate concentrations (Fig. 4C). Interestingly, butyrate production prior to the shift in inulin (i.e., day 2) was predictive of concentrations afterward (i.e., day 7), with only communities diluted 10^{-3} and 10^{-4} responding to higher inulin (Fig. 4D & Fig. S4C). Despite this variation in metabolic output, pH did not differ across dilutions when measured at day 10 (Fig. S4B). Our data suggest that, in our bioreactor system, a 10-fold inulin increase altered the functional output of the community with minimal effect on its composition, with more diluted communities not responding to that change. Four days after challenging with 10^5 vegetative *C. difficile* cells, reactors colonized to an average density of 10^6 CFU/mL *C. difficile* in the 10^{-5} and 10^{-6} groups (Fig. 4E). While all reactors had low initial levels of *C. difficile* colonization, only the communities in the 10^{-3} and 10^{-4} groups were able to ultimately prevent *C. difficile* invasion, suggesting that communities still able to respond to inulin also had the metabolic functions required to mediate

colonization resistance (Fig. 4E). While we observed a correlation between butyrate concentrations at day 0 and *C. difficile* colonization at day 4, butyrate did not affect *C. difficile* at the concentrations measured in our reactors in *in vitro* curves at pH 7 (Fig. S4D-F).

3. Discussion

The ability of an ecosystem to resist invasion by a non-indigenous species is tied to the diversity and temporal variability of community membership, an observation noted throughout the animal kingdom (27-30). Whether at the “macro” or “micro” levels of biology, environments provide a given set of nutrients to resident organisms, creating multi-dimensional niches comprised of biotic (e.g., nutrients, predators, etc.) and abiotic (eg., space, gas gradients, etc.) factors (31-36). The diversity and variability of a resident community determines how efficiently niches in the surrounding environment are utilized (36). In our study, we demonstrated that dilution of a community increases the variability of the established community, and those shifts are associated with *C. difficile* colonization resistance. However, this variability is only a marker of underlying metabolic interactions of colonization resistance as evidenced by an increase in resistance when we altered nutrient inputs into that environment.

These metabolic interactions manifest externally through greater competition with invaders as well as internally through limits placed on opportunistic taxa already present in that environment. Thus, we observed dilution having a two-fold disruptive effect on establishing communities, each tied to niche availability. First, while diversity is not strictly a metric of external stability, greater diversity allows for higher numbers of unique

interactions, both mutualistic and antagonistic, among community members (27, 37). These interactions increase the likelihood that spaces within a given niche become occupied through stronger cross-feeding interactions between resident members, which limits the invasion of foreign microbes (38-40). By removing rarer taxa, the stochastic nature of dilution weakened these interactions by destabilizing how the remaining microbes co-adapted to their new environment. The resulting changes decreased niche coverage by the resident microbiota (38). The resulting gaps reward microbes like *C. difficile*, which can adapt to use distinct niches depending on what is available in an environment (41). Additionally, networks of mutualistic and antagonistic interactions between microbes increase the likelihood of a microbial community's long-term survival (42). As observed in the communities that fully colonized with *C. difficile*, invasion by a foreign microbe triggered a collapse in the networks between resident organisms, resulting in their extinction (42).

Second, in addition to removing rarer taxa, dilution decreased the biomass of microbes starting off in each reactor. Since microbial abundance had recovered by the time of *C. difficile* challenge, we do not think that low microbial density played a direct role in the niches available to *C. difficile*. However, low microbial density left large open niches at the outset, which altered the early dynamics of community establishment. Microbes arrived in an environment absent of the competitors that previously had limited their expansion. This founder effect allowed opportunistic taxa within the resident community to take on outsized proportions due to their ability to use surrounding resources more efficiently (43, 44). Since the density of a seeding community regulates how they establish, it is inherently tied to how environmental niches become occupied (45). For

example, broad-spectrum antibiotic treatment induces significant gaps in niche coverage by reducing microbial abundance (46, 47). The downstream effects of these perturbations can linger for years, particularly if the event occurs early in the stages of microbial community development (e.g., in human infancy) (48). While perturbations that occur after a community reaches “maturity” have persistent effects, microbial communities tend to be impacted to a lesser extent (49, 50).

In our study, we also investigated the role of carbohydrates and microbial short-chain fatty acid metabolism in revealing the nature of altered community assembly affected by founder effects. While the metabolic nature of colonization resistance is multifactorial, several studies have characterized the role of SCFAs in limiting *C. difficile* establishment in the gut by altering the physiology of both microbe and host (23, 51, 52). While all SCFAs we measured can be products of inulin degradation, butyrate is relevant due to its toxicity to *C. difficile* as well as its ability to limit toxin-associated damage on the colonic epithelium (20, 51). While higher inulin concentrations induced an increase in butyrate, *C. difficile* tolerated those butyrate concentrations as measured by *in vitro* growth curves. Previous work suggests that SCFAs affect bacterial cells in a pH-dependent mechanism, with higher toxicity at lower pH due to the protonated acid form passing more easily through cellular membranes (53, 54). Our *in vitro* assays were balanced at pH 7, which limited toxicity that might be present in areas of the gut with lower pH and higher fermentative metabolic activity (32). Further research could disentangle the effects of butyrate on *C. difficile* physiology at unique pH levels (32).

Several studies have observed the presence of butyrogenic pathways in *C. difficile*, which may use butyrate as a terminal electron acceptor in the absence of other options,

such as Stickland amino acids (55-57). Due to unique toxicity patterns among the types of media used in our study as well as a previous study, we hypothesize that butyrate may have unique effects on *C. difficile* depending on which metabolic pathways are in use at the time of exposure (20, 58). This may be due in part to pressure from a build-up of downstream metabolic by-products as has been observed in *E. coli's* response to high concentrations of acetate and formate (59). Further work is required to characterize the specific effects of SCFAs on *C. difficile* physiology and potential impacts on virulence (53). In summary, if butyrate is one of the mediators of increased colonization resistance in the inulin-treated communities, our data suggest that it is acting in concert with other unknown mechanisms.

Understanding the establishment of microbes in a new environment is essential as we seek to develop defined consortia to treat microbiota-related gut conditions, such as *C. difficile* infection. Some of the limited success of certain consortia may be due in part to low seeding densities as well as the inadequacy of smaller consortia to cover the appropriate niche spaces. Keeping these ecological dynamics in mind will assist in creating reliable treatments with broader efficacy across a population.

4. Materials and Methods

4.1. Stool collection

This study was approved by the University of Michigan's Institutional Review Board (IRB: HUM00141992). We recruited adults (age > 18) and who had no history of gastrointestinal disease, including IBD, IBS, Crohn's Disease and cancer. Individuals also had no history of antibiotic use or intestinal infection (bacterial or viral) in the previous six

278 months. Exclusion criteria included immunocompromised status and immunosuppressant
279 use. Following informed consent, we provided enrolled subjects with a commode
280 specimen collection hat, and conical tubes, and instructions to freeze the stool sample, if
281 delivery and sample collection exceeded the given timeframe. Upon receipt of each
282 sample, we compensated subjects, and stored the sample at -80^{o}C until use. For the
283 experiments in this manuscript, we recruited two male individuals, aged 29 and 32.
284

285 **4.2. Bioreactor set-up and operation**

286 Through a collaboration with Robert Britton (Baylor University, Houston, TX), we
287 received three-dimensional designs for bioreactor strips, each containing six reactors
288 (14). With these designs, Protolabs, Inc. (Maple Plain, MN) used stereolithography to
289 create each bioreactor strip from a thermostable resin (Somos WaterShed XC 11122).
290 The operation of these bioreactor arrays has been previously described (14). Briefly, we
291 filled reactors with 15 mL of bioreactor media (BRM) prepared as previously described,
292 except that we sterilized bovine bile (Sigma, St. Louis, MO) by filtering at 0.22 µm (14).
293 Once we established continuous flow, multichannel Watson Marlow peristaltic pumps
294 (Falmouth, UK) individually maintained media flow to each reactor (1 rpm, 0.89 mm bore
295 tubing) at a rate of 0.13 mL/hr.
296

297 **4.3. Bioreactor dilution experiment**

298 To prepare the fecal inoculum, we suspended fecal content from Subject A in
299 sterile, pre-reduced phosphate-buffered saline (PBS; Thermo Fisher) at a ratio of 1:2.
300 Feces were serially diluted by 10-fold to 10^{-3}, 10^{-5}, 10^{-7}, and 10^{-9} in sterile, pre-reduced

PBS and established in reactors in sextuplicate (N = 4 for 10^{-3}). After 24 hrs of static culture, we initiated continuous flow and allowed to grow for 6 days before challenging with vegetative *Clostridioides difficile* str. 630 (Fig. 1A). Immediately before *C. difficile* challenge, we screened all reactors for possible contamination by plating on cycloserine-cefoxitin-fructose agar containing 0.1% taurocholate (TCCFA), which we made as previously described (60). To prepare *C. difficile* for challenge, we streaked spores onto agar plates containing taurocholate for 1 day at 37ºC under anaerobic conditions. After incubation, we inoculated a *C. difficile* colony into 10 mL of sterile, pre-reduced BRM. At approximately 16 hrs of incubation, we back-diluted 1 mL of the culture in BRM by 10-fold and monitored to ensure *C. difficile* was in a log-phase of growth. Upon reaching OD 0.1, we again back-diluted the *C. difficile* culture in BRM and then inoculated into each reactor. We took 1 mL samples from the reactors at days 0 (i.e., the start of flow), 2, 3, 6, 7, 9 and 10. We immediately pelleted cells, and transferred the supernatant to be stored separately at -80ºC. To assess *C. difficile* colonization, we enumerated colony-forming units (CFU) by serial dilution and plating on TCCFA.

4.4. Bioreactor carbohydrate experiment

To prepare the fecal inoculum, we suspended fecal content from Subject B in PBS as described above and then serially diluted to 10^{-3}, 10^{-4}, 10^{-5} and 10^{-6}. We established fecal dilutions into the bioreactors in triplicate. After 24 hrs of static culture, we established continuous flow using BRM (Fig. 4A). After 48 hrs of continuous flow, we switched source media for the reactors in each dilution group to BRM containing 10-fold higher inulin (Swanson, Fargo, ND) than standard BRM, increasing inulin concentrations from the

0.02% present in basal media to 0.2%. We held conditions for 5 days to give reactor communities time to establish before challenging with *C. difficile* on day 7 as described above. We took 1 mL samples at days 0, 2, 5, 6, 7, 8, 10 and 11. During sampling, we pelleted cells and transferred the supernatant to store at -80ºC. We then resuspended the pellet in RNAprotect Bacteria Reagent (Qiagen, Germantown, MD). We measured pH on day 10 of the experiment using MColorpHast pH test strips (Sigma).

4.5. DNA extraction and 16S rRNA-gene sequencing

We followed a detailed protocol for DNA extraction and Illumina MiSeq sequencing as described in previous publications with modifications (60). For the dilution bioreactor experiment, we pelleted cells and froze them at -80ºC. In preparation for sequencing, cells were bead beaten in molecular grade water using 0.1 mm silica beads for 2 minutes. We then submitted cell extracts to the University of Michigan Microbiome Core for sequencing. For the carbohydrate bioreactor experiment, we pelleted cells and resuspended in Qiagen RNAProtect Bacteria Reagent before storing at -80ºC. In preparation for sequencing, we submitted samples to the University of Michigan Microbiome Core for extraction using the Qiagen MagAttract PowerMicrobiome DNA/RNA Isolation Kit. For both experiments, we randomized samples into each extraction plate. To amplify the DNA, we used barcoded dual-index primers specific to the V4 region of the 16S rRNA-gene, and ran negative and positive controls in each sequencing plate (61). We prepared and sequenced libraries using the 500-cycle MiSeq V2 reagent kit (Illumina, San Diego, CA). Raw FASTQ files were deposited in the Sequence Read Archive (SRA) database (BioProject Accession: PRJNA837590).

4.6. Data processing and microbiota analysis

We performed 16S rRNA-gene sequencing as previously described using the V4 variable region and analyzed using mothur (62). Detailed methods, processed read data and the data analysis are described on GitHub (https://github.com/mschnizlein/cdiff_foundereffects). Briefly, after initial steps, such as assembly and quality control, we aligned contigs to the Silva v. 138 16S rRNA database (63). We removed chimeras using UCHIME and excluded samples with less than 1000 sequences (64). We binned contigs into operational taxonomic units (OTUs) by 97% percent similarity using Opticlust and used the Silva rRNA sequence database to classify those sequences (63, 65). Alpha and beta diversity metrics were calculated from unfiltered OTU samples. After subsampling to 2000 sequences, we used Dirichlet Multinomial Modelling (DMM) to identify bacterial enterotypes based on genus-level classification and then used LEfSe to identify taxa that significantly associate with each of these community types (66, 67). We performed all statistical analyses in R (v. 4.1.1) using the following packages: ggplot2, reshape2, plyr, tidyverse, ComplexHeatmap, and scales (68-73).

4.7. 16S rRNA-gene qPCR

Using dilutions of *Escherichia coli* ECOR2 genomic DNA as standards, we performed qPCR using PrimeTime gene expression master mix (IDT, Coralville, IA) and a set of broad-range 16S rRNA gene primers on a Thermo Fisher QuantStudio 3 (74). The DNA samples, standards, and negative controls were all amplified in triplicate. The

370 qPCR reaction conditions were as follows: 95°C for 3 min, followed by 40 cycles of two-
371 step amplification at 95°C for 15 s and 60°C for 60 s. The quantification cycle (Cq) values
372 for each reaction were determined by using the Thermo Fisher Cloud software, and
373 sample DNA concentrations were determined by comparing Cq values to the standards
374 in each plate.
375
376 **4.8. *C. difficile* growth curves**
377 We isolated *C. difficile* strain 630g from a spore stock by growing overnight on BHI
378 agar (BD) supplemented with 0.01% L-cysteine hydrochloride monohydrate (BHI; Sigma)
379 and 0.1% taurocholate (Sigma). Growth curves were conducted with two biological
380 replicates grown from two unique colonies. After growing overnight in BHI, we back-
381 diluted cultures in fresh BHI with the overnight sample, and optical density was monitored
382 to ensure cultures were in log-phase growth. Prior to the growth assay, we pelleted the
383 culture, and then resuspended it in fresh 2x concentration BHI. We mixed this bacterial
384 suspension into sodium butyrate solutions buffered at pH 7 with PBS ranging from 160mM
385 to 2.5mM (2x final concentrations). The cultures were then placed in a 96-well plate optical
386 density reader (Tecan, Switzerland) and monitored for 24 hours. All conditions were run
387 with three technical replicates. Optical density measurements at 600 nm were
388 automatically taken every 15 min, with 60 s of shaking immediately prior to measurement.
389 We repeated this protocol in a follow-up experiment but substituted BHI for BRM in all
390 steps following *C. difficile* colony isolation.
391
392 **4.9. Short-chain fatty acid analysis**

393 100 uL of fecal supernatants were filtered using 0.22 micron 96-well filter plates
394 and stored at -20^{o}C until analysis. We transferred the filtrate to 1.5 mL screw cap vials
395 with 100 uL inserts for high performance liquid chromatography (HPLC) analysis and then
396 randomized them. We quantified acetate, propionate, and butyrate concentrations using
397 a refractive index detector as part of a Shimadzu HPLC system (Shimadzu Scientific
398 Instruments, Columbia, MD) as previously described (75). Briefly, we used a 0.01 N
399 H_2SO_4 mobile phase in filtered, Milli-Q water through an Aminex HPX87H column (Bio-
400 Rad Laboratories, Hercules, CA). Sample areas under the curve were compared to
401 volatile fatty acid standards with concentrations of 40, 20, 10, 5, 2.5, 1, 0.5, 0.25, and 0.1
402 mM. Through blinded curation, we assessed baseline and peak quality and excluded poor
403 quality data if necessary.
404
405
406

References:

1. Zmora N, Zilberman-Schapira G, Suez J, Mor U, Dori-Bachash M, Bashiardes S, Kotler E, Zur M, Regev-Lehavi D, Brik RB-Z, Federici S, Cohen Y, Linevsky R, Rothschild D, Moor AE, Ben-Moshe S, Harmelin A, Itzkovitz S, Maharshak N, Shibolet O, Shapiro H, Pevsner-Fischer M, Sharon I, Halpern Z, Segal E, Elinav E. 2018. Personalized gut mucosal colonization resistance to empiric probiotics is associated with unique host and microbiome features. Cell 174:1388-1405.e21.
2. Parlet CP, Brown MM, Horswill AR. 2019. Commensal staphylococci influence *Staphylococcus aureus* skin colonization and disease. Trends Microbiol 27:497-507.
3. Crouzet L, Rigottier-Gois L, Serror P. 2015. Potential use of probiotic and commensal bacteria as non-antibiotic strategies against vancomycin-resistant enterococci. FEMS Microbiol Letters 362:fnv012.
4. Ducarmon QR, Zwittink RD, Hornung BVH, van Schaik W, Young VB, Kuijper EJ. 2019. Gut microbiota and colonization resistance against bacterial enteric infection. Microbiol Mol Biol Rev 83.
5. Aranda-Díaz A, Ng KM, Thomsen T, Real-Ramírez I, Dahan D, Dittmar S, Gonzalez CG, Chavez T, Vasquez KS, Nguyen TH, Yu FB, Higginbottom SK, Neff NF, Elias JE, Sonnenburg JL, Huang KC. 2022. Establishment and characterization of stable, diverse, fecal-derived in vitro microbial communities that model the intestinal microbiota. Cell Host Microbe 30:260-272.e5.
6. Chilton CH, Crowther GS, Baines SD, Todhunter SL, Freeman J, Locher HH, Athanasiou A, Wilcox MH. 2014. *In vitro* activity of cadazolid against clinically relevant *Clostridium difficile* isolates and in an in vitro gut model of *C. difficile* infection. J Antimicrob Chemother 69:697-705.
7. Davies M, Galazzo G, van Hattem JM, Arcilla MS, Melles DC, de Jong MD, Schultsz C, Wolffs P, McNally A, Schaik WV, Penders J. 2022. Enterobacteriaceae and Bacteroidaceae provide resistance to travel-associated intestinal colonization by multi-drug resistant *Escherichia coli*. Gut Microbes 14:2060676.
8. Li Q, Chen S, Zhu K, Huang X, Huang Y, Shen Z, Ding S, Gu D, Yang Q, Sun H, Hu F, Wang H, Cai J, Ma B, Zhang R, Shen J. 2022. Collateral sensitivity to pleuromutilins in vancomycin-resistant *Enterococcus faecium*. Nat Commun 13:1888.
9. Pérez Escriva P, Fuhrer T, Sauer U. 2022. Distinct N and C cross-feeding networks in a synthetic mouse gut consortium. mSystems doi:10.1128/msystems.01484-21:e0148421.
10. Reed AD, Fletcher JR, Huang YY, Thanissery R, Rivera AJ, Parsons RJ, Stewart AK, Kountz DJ, Shen A, Balskus EP, Theriot CM. 2022. The stickland reaction precursor *trans*-4-hydroxy-l-proline differentially impacts the metabolism of *Clostridioides difficile* and commensal clostridia. mSphere doi:10.1128/msphere.00926-21:e0092621.
11. Rajan A, Robertson MJ, Carter HE, Poole NM, Clark JR, Green SI, Criss ZK, Zhao B, Karandikar U, Xing Y, Margalef-Català M, Jain N, Wilson RL, Bai F, Hyser JM, Petrosino J, Shroyer NF, Blutt SE, Coarfa C, Song X, Prasad BV, Amieva MR, Grande-Allen J, Estes MK, Okhuysen PC, Maresso AW. 2020. Enteroaggregative

E. coli Adherence to Human Heparan Sulfate Proteoglycans Drives Segment and Host Specific Responses to Infection. PLOS Pathogens 16:e1008851.

12. Engevik MA, Danhof HA, Shrestha R, Chang-Graham AL, Hyser JM, Haag AM, Mohammad MA, Britton RA, Versalovic J, Sorg JA, Spinler JK. 2020. Reuterin disrupts *Clostridioides difficile* metabolism and pathogenicity through reactive oxygen species generation. Gut Microbes 12:1788898.
13. Gonyar LA, Smith RM, Giron JA, Zachos NC, Ruiz-Perez F, Nataro JP. 2020. Aggregative adherence fimbriae II of enteroaggregative *Escherichia coli* are required for adherence and barrier disruption during infection of human colonoids. Infect Immun 88.
14. Auchtung JM, Robinson CD, Farrell K, Britton RA. 2016. MiniBioReactor Arrays (MBRAs) as a tool for studying *C. difficile* physiology in the presence of a complex community. Methods Mol Biol 1476:235-58.
15. Freeman J, O'Neill FJ, Wilcox MH. 2003. Effects of cefotaxime and desacetylcefotaxime upon *Clostridium difficile* proliferation and toxin production in a triple-stage chemostat model of the human gut. J Antimicrob Chemother 52.
16. Freeman J, Baines SD, Jabes D, Wilcox MH. 2005. Comparison of the efficacy of ramoplanin and vancomycin in both *in vitro* and *in vivo* models of clindamycin-induced *Clostridium difficile* infection. J Antimicrob Chemother 56:717-25.
17. Baines SD, Freeman J, Wilcox MH. 2005. Effects of piperacillin/tazobactam on *Clostridium difficile* growth and toxin production in a human gut model. J Antimicrob Chemother 55:974-82.
18. Zackular JP, Moore JL, Jordan AT, Juttukonda LJ, Noto MJ, Nicholson MR, Crews JD, Semler MW, Zhang Y, Ware LB, Washington MK, Chazin WJ, Caprioli RM, Skaar EP. 2016. Dietary zinc alters the microbiota and decreases resistance to *Clostridium difficile* infection. Nat Med 22:1330-1334.
19. Ward P, P. Young G. 1997. Dynamics of *Clostridium difficile* infection: Control using diet, vol 412.
20. Hryckowian AJ, Van Treuren W, Smits SA, Davis NM, Gardner JO, Bouley DM, Sonnenburg JL. 2018. Microbiota-accessible carbohydrates suppress *Clostridium difficile* infection in a murine model. Nat Microbiol 3:662-669.
21. Auchtung JM, Robinson CD, Britton RA. 2015. Cultivation of stable, reproducible microbial communities from different fecal donors using minibioreactor arrays (MBRAs). Microbiome 3:42.
22. Auchtung JM, Preisner EC, Collins J, Lerma AI, Britton RA, Young VB. 2020. Identification of simplified microbial communities that inhibit *Clostridioides difficile* infection through dilution/extinction. mSphere 5:e00387-20.
23. Seekatz AM, Theriot CM, Rao K, Chang Y-M, Freeman AE, Kao JY, Young VB. 2018. Restoration of short chain fatty acid and bile acid metabolism following fecal microbiota transplantation in patients with recurrent *Clostridium difficile* infection. Anaerobe doi:10.1016/j.anaerobe.2018.04.001.
24. Yang J, Martínez I, Walter J, Keshavarzian A, Rose DJ. 2013. *In vitro* characterization of the impact of selected dietary fibers on fecal microbiota composition and short chain fatty acid production. Anaerobe 23:74-81.

25. Van den Abbeele P, Venema K, Van de Wiele T, Verstraete W, Possemiers S. 2013. Different human gut models reveal the distinct fermentation patterns of arabinoxylan versus inulin. J Agric Food Chem 61:9819-27.
26. Valcheva R, Koleva P, Martínez I, Walter J, Gänzle MG, Dieleman LA. 2019. Inulin-type fructans improve active ulcerative colitis associated with microbiota changes and increased short-chain fatty acids levels. Gut Microbes 10:334-357.
27. Qian JJ, Akçay E. 2020. The balance of interaction types determines the assembly and stability of ecological communities. Nat Ecol Evol 4:356-365.
28. Song C, Uricchio LH, Mordecai EA, Saavedra S. 2021. Understanding the emergence of contingent and deterministic exclusion in multispecies communities. Ecol Lett 24:2155-2168.
29. Morris JR, Allhoff KT, Valdovinos FS. 2021. Strange invaders increase disturbance and promote generalists in an evolving food web. Sci Rep 11:21274.
30. Wang C, Cheng H, Wang S, Wei M, Du D. 2021. Plant community and the influence of plant taxonomic diversity on community stability and invasibility: A case study based on Solidago canadensis L. Sci Total Environ 768:144518.
31. Konjar Š, Pavšič M, Veldhoen M. 2021. Regulation of oxygen homeostasis at the intestinal epithelial barrier site. Int J Mol Sci 22.
32. Wetzel D, McBride SM. 2020. The impact of pH on *Clostridioides difficile* sporulation and physiology. Appl Environ Microbiol 86.
33. Djemai K, Drancourt M, Tidjani Alou M. 2021. Bacteria and methanogens in the human microbiome: A review of syntrophic interactions. Microb Ecol doi:10.1007/s00248-021-01796-7.
34. Pereira FC, Berry D. 2017. Microbial nutrient niches in the gut. Environ Microbiol 19:1366-1378.
35. Bono LM, Draghi JA, Turner PE. 2020. Evolvability costs of niche expansion. Trends Genet 36:14-23.
36. Baquero F, Coque TM, Galán JC, Martinez JL. 2021. The origin of niches and species in the bacterial world. Frontiers in Microbiology 12.
37. Vila JCC, Jones ML, Patel M, Bell T, Rosindell J. 2019. Uncovering the rules of microbial community invasions. Nature Ecology & Evolution 3:1162-1171.
38. Badali M, Zilman A. 2020. Effects of niche overlap on coexistence, fixation and invasion in a population of two interacting species. R Soc Open Sci 7:192181.
39. Herren CM. 2020. Disruption of cross-feeding interactions by invading taxa can cause invasional meltdown in microbial communities. Proc Biol Sci 287:20192945.
40. Diaz-Colunga J, Lu N, Sanchez-Gorostiaga A, Chang CY, Cai HS, Goldford JE, Tikhonov M, Sánchez Á. 2022. Top-down and bottom-up cohesiveness in microbial community coalescence. Proc Natl Acad Sci USA 119.
41. Jenior ML, Leslie JL, Young VB, Schloss PD. 2017. *Clostridium difficile* colonizes alternative nutrient niches during infection across distinct murine gut microbiomes. mSystems 2.
42. Bascompte J, Stouffer DB. 2009. The assembly and disassembly of ecological networks. Philosophical Transactions of the Royal Society B: Biological Sciences 364:1781-1787.
43. Brown SP, Cornforth DM, Mideo N. 2012. Evolution of virulence in opportunistic pathogens: generalism, plasticity, and control. Trends Microbiol 20:336-342.

44. Sheppard SK. 2022. Strain wars and the evolution of opportunistic pathogens. Current Opinion in Microbiology 67:102138.
45. Waters JM, Fraser CI, Hewitt GM. 2013. Founder takes all: Density-dependent processes structure biodiversity. Trends in Ecology & Evolution 28:78-85.
46. Dethlefsen L, Relman DA. 2011. Incomplete recovery and individualized responses of the human distal gut microbiota to repeated antibiotic perturbation. Proc Natl Acad Sci USA 108 Suppl 1:4554-61.
47. Schubert AM, Sinani H, Schloss PD. 2015. Antibiotic-induced alterations of the murine gut microbiota and subsequent effects on colonization resistance against *Clostridium difficile*. mBio 6:e00974-15.
48. Korpela K, Salonen A, Virta LJ, Kekkonen RA, Forslund K, Bork P, de Vos WM. 2016. Intestinal microbiome is related to lifetime antibiotic use in Finnish pre-school children. Nat Commun 7:10410.
49. Dethlefsen L, Huse S, Sogin ML, Relman DA. 2008. The pervasive effects of an antibiotic on the human gut microbiota, as revealed by deep 16S rRNA sequencing. PLOS Biology 6:e280.
50. Jernberg C, Löfmark S, Edlund C, Jansson JK. 2007. Long-term ecological impacts of antibiotic administration on the human intestinal microbiota. ISME J 1:56-66.
51. Fachi JL, Felipe JdS, Pral LP, da Silva BK, Corrêa RO, de Andrade MCP, da Fonseca DM, Basso PJ, Câmara NOS, de Sales e Souza ÉL, dos Santos Martins F, Guima SES, Thomas AM, Setubal JC, Magalhães YT, Forti FL, Candreva T, Rodrigues HG, de Jesus MB, Consonni SR, Farias AdS, Varga-Weisz P, Vinolo MAR. 2019. Butyrate protects mice from *Clostridium difficile*-induced colitis through an HIF-1-dependent mechanism. Cell Reports 27:750-761.e7.
52. Gregory AL, Pensinger DA, Hryckowian AJ. 2021. A short chain fatty acid-centric view of *Clostridioides difficile* pathogenesis. PLOS Pathogens 17:e1009959.
53. Sun Y, O'Riordan MXD. 2013. Regulation of bacterial pathogenesis by intestinal short-chain fatty acids. Advances in Applied Microbiology 85:93-118.
54. Cherrington CA, Hinton M, Mead GC, Chopra I. 1991. Organic acids: Chemistry, antibacterial activity and practical applications, p 87-108. *In* Rose AH, Tempest DW (ed), Advances in Microbial Physiology, vol 32. Academic Press.
55. Mullany P, Clayton CL, Pallen MJ, Slone R, al-Saleh A, Tabaqchali S. 1994. Genes encoding homologues of three consecutive enzymes in the butyrate/butanol-producing pathway of *Clostridium acetobutylicum* are clustered on the *Clostridium difficile* chromosome. FEMS Microbiol Letters 124:61-7.
56. Aboulnaga el H, Pinkenburg O, Schiffels J, El-Refai A, Buckel W, Selmer T. 2013. Effect of an oxygen-tolerant bifurcating butyryl coenzyme A dehydrogenase/electron-transferring flavoprotein complex from *Clostridium difficile* on butyrate production in *Escherichia coli*. J Bacteriol 195:3704-13.
57. Gencic S, Grahame DA. 2020. Diverse energy-conserving pathways in *Clostridium difficile*: Growth in the absence of amino acid Stickland acceptors and the role of the Wood-Ljungdahl Pathway. J Bacteriol 202.
58. Karasawa T, Ikoma S, Yamakawa K, Nakamura S. 1995. A defined growth medium for *Clostridium difficile*. Microbiology 141:371-375.

59. Kirkpatrick C, Maurer LM, Oyelakin NE, Yoncheva YN, Maurer R, Slonczewski JL. 2001. Acetate and formate stress: Opposite responses in the proteome of *Escherichia coli*. J of Bacteriology 183:6466-6477.
60. Leslie JL, Vendrov KC, Jenior ML, Young VB. 2019. The gut microbiota is associated with clearance of *Clostridium difficile* infection independent of adaptive immunity. mSphere 4:e00698-18.
61. Kozich JJ, Westcott SL, Baxter NT, Highlander SK, Schloss PD. 2013. Development of a dual-index sequencing strategy and curation pipeline for analyzing amplicon sequence data on the MiSeq Illumina sequencing platform. Appl Environ Microbiol 79.
62. Schloss PD, Westcott SL, Ryabin T, Hall JR, Hartmann M, Hollister EB, Lesniewski RA, Oakley BB, Parks DH, Robinson CJ, Sahl JW, Stres B, Thallinger GG, Van Horn DJ, Weber CF. 2009. Introducing mothur: Open-source, platform-independent, community-supported software for describing and comparing microbial communities. Appl Environ Microbiol 75:7537-41.
63. Pruesse E, Quast C, Knittel K, Fuchs BM, Ludwig W, Peplies J, Glockner FO. 2007. SILVA: a comprehensive online resource for quality checked and aligned ribosomal RNA sequence data compatible with ARB. Nucleic Acids Res 35:7188-96.
64. Edgar RC, Haas BJ, Clemente JC, Quince C, Knight R. 2011. UCHIME improves sensitivity and speed of chimera detection. Bioinformatics 27:2194-200.
65. Westcott SL, Schloss PD. 2017. OptiClust, an improved method for assigning amplicon-based sequence data to operational taxonomic units. mSphere 2.
66. Holmes I, Harris K, Quince C. 2012. Dirichlet multinomial mixtures: Generative models for microbial metagenomics. PLOS ONE 7:e30126.
67. Segata N, Izard J, Waldron L, Gevers D, Miropolsky L, Garrett WS, Huttenhower C. 2011. Metagenomic biomarker discovery and explanation. Genome Biology 12:R60-R60.
68. Team RC. 2013. R: A language and environment for statistical computing. R Foundation for Statistical Computing.
69. Wickham H. 2016. ggplot2: Elegant graphics for data analysis. Springer-Verlag, New York.
70. Wickham H. 2007. Reshaping data with the reshape package. J of Statistical Software 21:1 - 20.
71. Wickham H. 2011. The split-apply-combine strategy for data analysis. J of Statistical Software 40:1 - 29.
72. Wickham H, Averick M, Bryan J, Chang W, McGowan LDA, François R, Grolemund G, Hayes A, Henry L, Hester J, Kuhn M, Pedersen TL, Miller E, Bache SM, Müller K, Ooms J, Robinson D, Seidel DP, Spinu V, Takahashi K, Vaughan D, Wilke C, Woo K, Yutani H. 2019. Welcome to the Tidyverse. J of Open Source Software 4.
73. Gu Z, Eils R, Schlesner M. 2016. Complex heatmaps reveal patterns and correlations in multidimensional genomic data. Bioinformatics 32:2847-9.
74. Nadkarni MA, Martin FE, Jacques NA, Hunter N. 2002. Determination of bacterial load by real-time PCR using a broad-range (universal) probe and primers set. Microbiology 148:257-266.

633 75. Baxter NT, Schmidt AW, Venkataraman A, Kim KS, Waldron C, Schmidt TM. 2019.
634 Dynamics of human gut microbiota and short-chain fatty acids in response to
635 dietary interventions with three fermentable fibers. mBio 10:e02566-18.
636 -

637

638

639

Figure 1: Establishment dynamics of diluted microbial communities. A) Experimental timeline of the bioreactor dilution experiment. **B)** Observed species (SOBS) is plotted by dilution from day 0 to the day of *C. difficile* challenge. **C)** Principal coordinate analysis of all timepoints in each community dilution (ellipses represent the 95% confidence interval of a multivariate t-distribution for datapoints in each dilution). **D-G)** Averaged relative abundance at each indicated timepoint for the communities diluted **D)** 10^{-3}, **E)** 10^{-5}, **F)** 10^{-7}, and **G)** 10^{-9}. Taxa are color coded and ordered by phylum (Bacteroidota = green, Bacillota = blue/purple, Actinomycetota = orange, Pseudomonadota = red and Verrucomicrobiota = yellow. Other phyla, low abundance taxa and unclassified bacteria are colored as grey).

Figure 2: Intra-group community variability by dilution. Intra-group β-diversity was compared across samples for each of the four community dilution groups using the **A)** Bray-Curtis Dissimilarity Index and the **B)** Jaccard Dissimilarity Index (statistical analysis: one-way ANOVA).

Figure 3: Associations between *C. difficile* colonization and microbiota community type. A) *C. difficile* colonization on each day following challenge measured in CFU/mL (dashed line = limit of detection). **B)** All samples were categorized into three unique community types by Dirichlet Multinomial Modelling (DMM). Their relative abundance in each dilution group is plotted with the total number of samples in each dilution listed on the x-axis (statistical analysis: Fisher's Exact Test). **C)** *C. difficile* abundance in each sample is compared to that samples associated community type (statistical analysis: Wilcoxon Rank Sum Test, * indicates $p < 0.01$). **D)** Average relative abundance of bacterial taxa in each community type (Peptostreptococcales is abbreviated as Peptostr.; Bacteroidota = green, Bacillota = blue/purple, Actinomycetota = orange, Pseudomonadota = red, Verrucomicrobiota = yellow and Desulfovibrio = grey. Other phyla, low abundance taxa and unclassified bacteria are colored as black).

Figure 4: Effect of inulin on microbial community function. **A)** Experimental timeline of the bioreactor carbohydrate experiment. **B)** Observed species (SOBS) over time colored by dilution group (statistical analysis: Kruskal-Wallis Test comparing SOBS at all timepoints with dilution group, $p < 0.01$; Wilcoxon Rank Sum Test comparing OTUs in each group at day 2 and day 5, p = not significant). **C)** Short chain fatty acid concentrations in the 0.2% inulin group as measured by HPLC from day 2 (pre-media switch) and day 7 (5 days post-media switch; Ac = acetate, Pr = propionate, Bu = butyrate; statistical analysis: Wilcoxon Rank Sum Test, * indicates $p < 0.01$ and a indicates $p = 0.033$). **D)** Butyrate response 3 and 5 days following the shift to higher inulin, with communities being colored by dilution (statistical analysis: at day 7, 10^{-3} and 10^{-4} compared to 10^{-5} and 10^{-6} using the Wilcoxon Rank Sum Test, * indicates $p < 0.01$). **E)** *C. difficile* colonization in the reactors treated with 0.2% inulin, colored by community dilution (dashed line = limit of detection).

Figure S1: Individualized establishment dynamics of diluted microbial communities. A) Observed species (SOBS) from all timepoints are plotted by community dilution. **B)** 16S rRNA-gene copies on days 0 and 6 are plotted by dilution. **C-F)** Relative

686 abundance of 16S rRNA gene sequences is plotted for each individual reactor in the
687 communities diluted **C)** 10^{-3}, **D)** 10^{-5}, **E)** 10^{-7}, and **F)** 10^{-9} (Bacteroidota = green, Firmicutes
688 = blue/purple, Actinobacteriota = orange, Proteobacteriota = red and Verrucomicrobiota
689 = yellow. Other phyla, low abundance taxa and unclassified bacteria are colored as grey).
690
691 **Figure S2: Intra-reactor community variability by dilution.** Intra-reactor β-diversity
692 was compared across samples within each reactor for the four community dilution groups
693 using the **A)** Bray-Curtis Dissimilarity Index and the **B)** Jaccard Dissimilarity Index
694 (statistical analysis: one-way ANOVA).
695
696 **Figure S3: Associations between *C. difficile* and resident microbes. A)** Observed
697 species (SOBS) in each community dilution following *C. difficile* challenge. *C. difficile*
698 abundance compared to the SOBS on **B)** day 6 and **C)** day 7 (statistical analysis: linear
699 regression). LEfSe analysis comparing bacterial taxa in community types 1 & 3 with those
700 in type 2. Certain taxa were more abundant in **D)** types 1 & 3 and others in **E)** type 2.
701
702 **Figure S4: Effects of inulin on microbial community function. A)** Bray-Curtis
703 Dissimilarity index of communities in the 0.2% inulin treated reactor groups colored by
704 dilution. Each point represents the distance of each reactor community relative to its
705 baseline at day 0 (statistical analysis: Wilcoxon Rank Sum Test comparing distance to
706 baseline at day 2 and day 5; for 10^{-3}, $p = 0.016$; for 10^{-4}, 10^{-5} and 10^{-6}, p = not significant).
707 **B)** pH of each reactor by dilution group at day 10 (statistical test: Kruskal-Wallis test). **C)**
708 Butyrate concentrations at day 2 (pre-inulin shift) compared to concentrations at day 7
709 (statistical analysis: linear regression). **D)** Butyrate concentrations at day 7 compared to
710 *C. difficile* colonization on day 11. *C. difficile* growth curves in assessing butyrate toxicity
711 in **E)** BHI and **F)** BRM, each buffered at pH 7.
712

713

Acknowledgements: We would like to thank the Microbial Systems and Molecular Biology Core at the University of Michigan for their work performing the DNA extractions and 16S rRNA-gene sequencing. Many thanks go to Deanna Montgomery for critical review of this manuscript. We would also like to thank Thomas Schmidt and Kwi Kim for their guidance performing the HPLC short chain fatty acid analysis. Finally, we thank members of the Robert Britton lab for assistance as we got the bioreactor model running in the lab. This work was funded by the National Institutes for Allergy and Infectious Disease (U01-AI124255) and for Diabetes and Digestive and Kidney Diseases (T32-DK094775).

Contributions:

M.K.S.: Conceptualization, data curation, formal analysis, investigation, methodology, project administration, visualization, writing (original draft), writing (review & editing)

A.K.S.: investigation, methodology, writing (review & editing)

M.J.G.: investigation, formal analysis, visualization, writing (review & editing)

S.J.E.: investigation, formal analysis, writing (review & editing)

V.B.Y.: Conceptualization, funding acquisition, project administration, resources, supervision, writing (original draft), writing (review & editing)

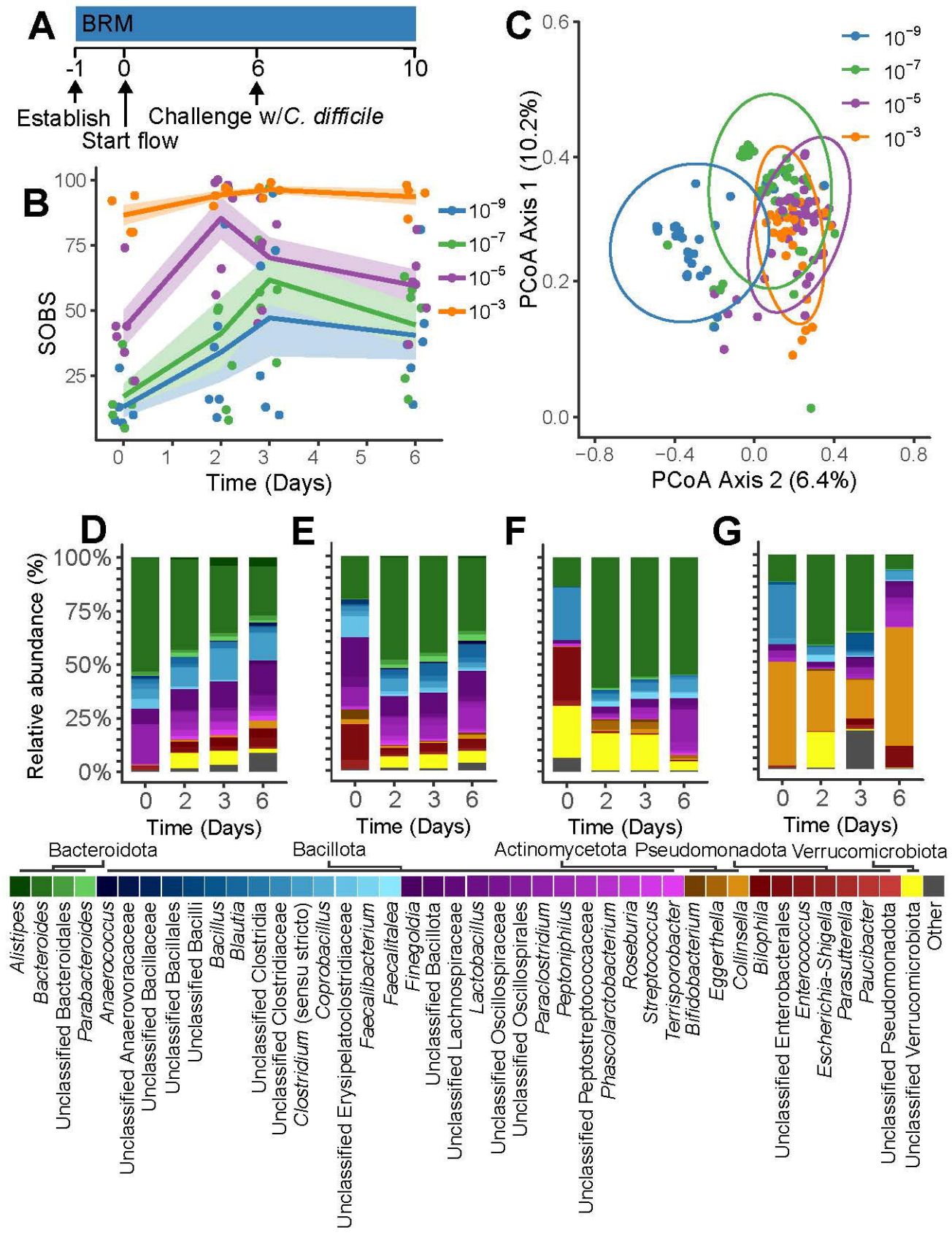
A
BRM
-1
0
6
10
Establish
Start flow
Challenge w/C. difficile
B
SOBS
Time (Days)
10^{-9}
10^{-7}
10^{-5}
10^{-3}
C
PCoA Axis 1 (10.2%)
PCoA Axis 2 (6.4%)
D
E
F
G
Relative abundance (%)
Bacteroidota
Bacillota
Actinomycetota
Pseudomonadota
Verrucomicrobiota
Alistipes
Bacteroides
Unclassified Bacteroidales
Parabacteroides
Anaerococcus
Unclassified Anaerovoracaceae
Unclassified Bacillaceae
Unclassified Bacillales
Unclassified Bacilli
Bacillus
Blautia
Unclassified Clostridia
Unclassified Clostridiaceae
Clostridium (sensu stricto)
Coprobacillus
Unclassified Erysipelatoclostridiaceae
Faecalibacterium
Faecalitalea
Finegoldia
Unclassified Bacillota
Unclassified Lachnospiraceae
Lactobacillus
Unclassified Oscillospiraceae
Unclassified Oscillospirales
Paraclostridium
Peptoniphilus
Unclassified Peptostreptococcaceae
Phascolarctobacterium
Roseburia
Streptococcus
Terrisporobacter
Bifidobacterium
Eggerthella
Collinsella
Bilophila
Unclassified Enterobacterales
Enterococcus
Escherichia-Shigella
Parasutterella
Paucibacter
Unclassified Pseudomonadota
Unclassified Verrucomicrobiota
Other

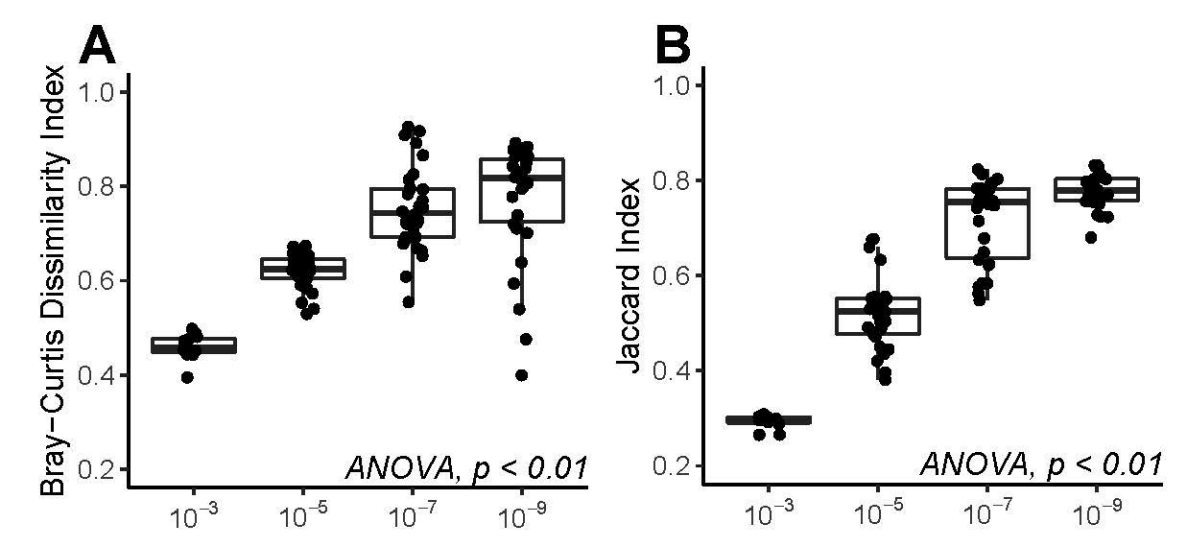
A
Bray–Curtis Dissimilarity Index
1.0
0.8
0.6
0.4
0.2
ANOVA, p < 0.01
10^-3
10^-5
10^-7
10^-9
B
Jaccard Index
1.0
0.8
0.6
0.4
0.2
ANOVA, p < 0.01
10^-3
10^-5
10^-7
10^-9

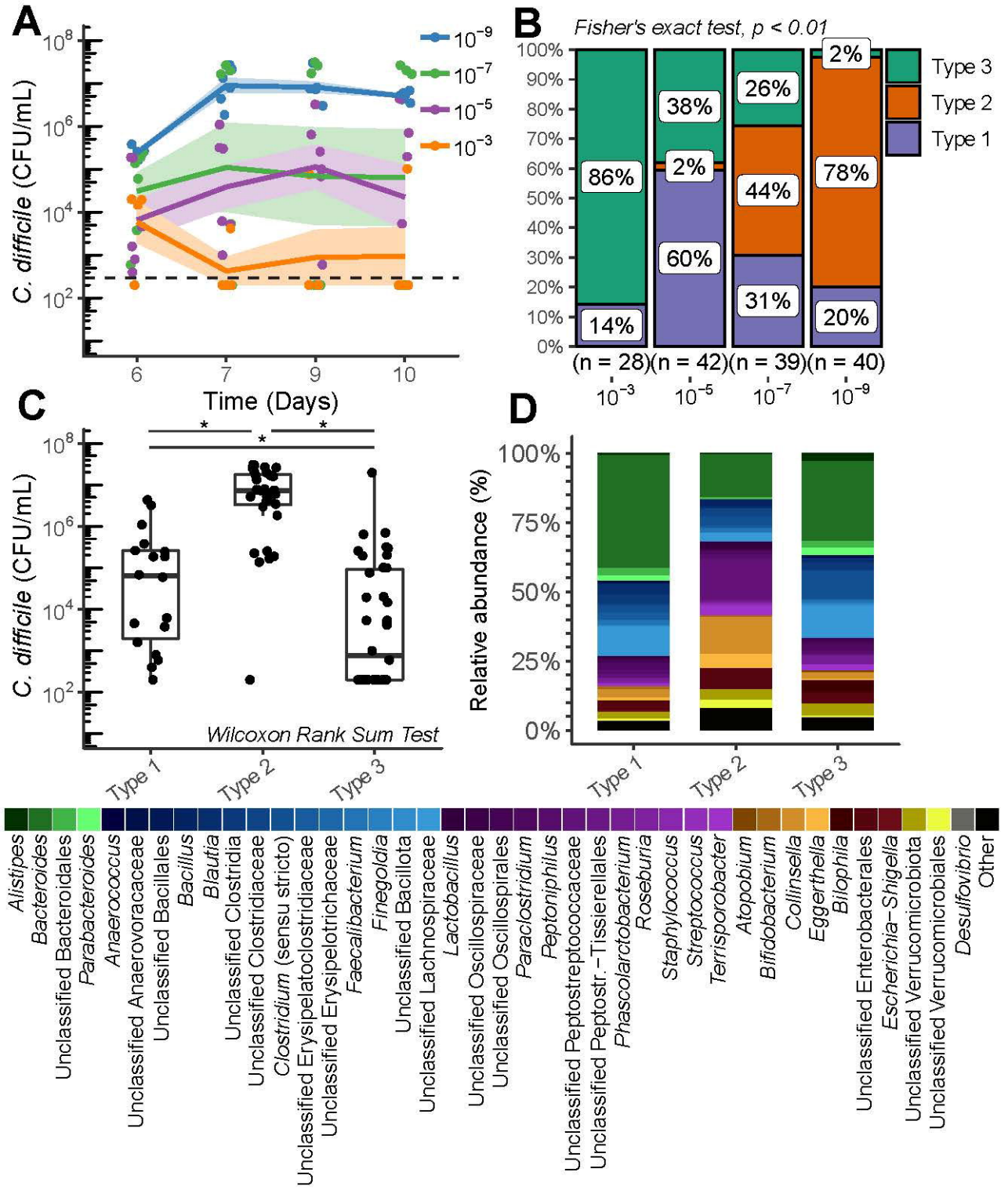
A
C. difficile (CFU/mL)
Time (Days)
10^-9
10^-7
10^-5
10^-3
B
Fisher's exact test, p < 0.01
Type 3
Type 2
Type 1
86%
14%
38%
2%
60%
26%
44%
31%
2%
78%
20%
(n = 28)
(n = 42)
(n = 39)
(n = 40)
C
Wilcoxon Rank Sum Test
Type 1
Type 2
Type 3
D
Relative abundance (%)
Alistipes
Bacteroides
Unclassified Bacteroidales
Parabacteroides
Anaerococcus
Unclassified Anaerovoracaceae
Unclassified Bacillales
Bacillus
Blautia
Unclassified Clostridia
Unclassified Clostridiaceae
Clostridium (sensu stricto)
Unclassified Erysipelatoclostridiaceae
Unclassified Erysipelotrichaceae
Faecalibacterium
Finegoldia
Unclassified Bacillota
Unclassified Lachnospiraceae
Lactobacillus
Unclassified Oscillospiraceae
Unclassified Oscillospirales
Paraclostridium
Peptoniphilus
Unclassified Peptostreptococcaceae
Unclassified Peptostr.-Tissierellales
Phascolarctobacterium
Roseburia
Staphylococcus
Streptococcus
Terrisporobacter
Atopobium
Bifidobacterium
Collinsella
Eggerthella
Bilophila
Unclassified Enterobacterales
Escherichia-Shigella
Unclassified Verrucomicrobiota
Unclassified Verrucomicrobiales
Desulfovibrio
Other

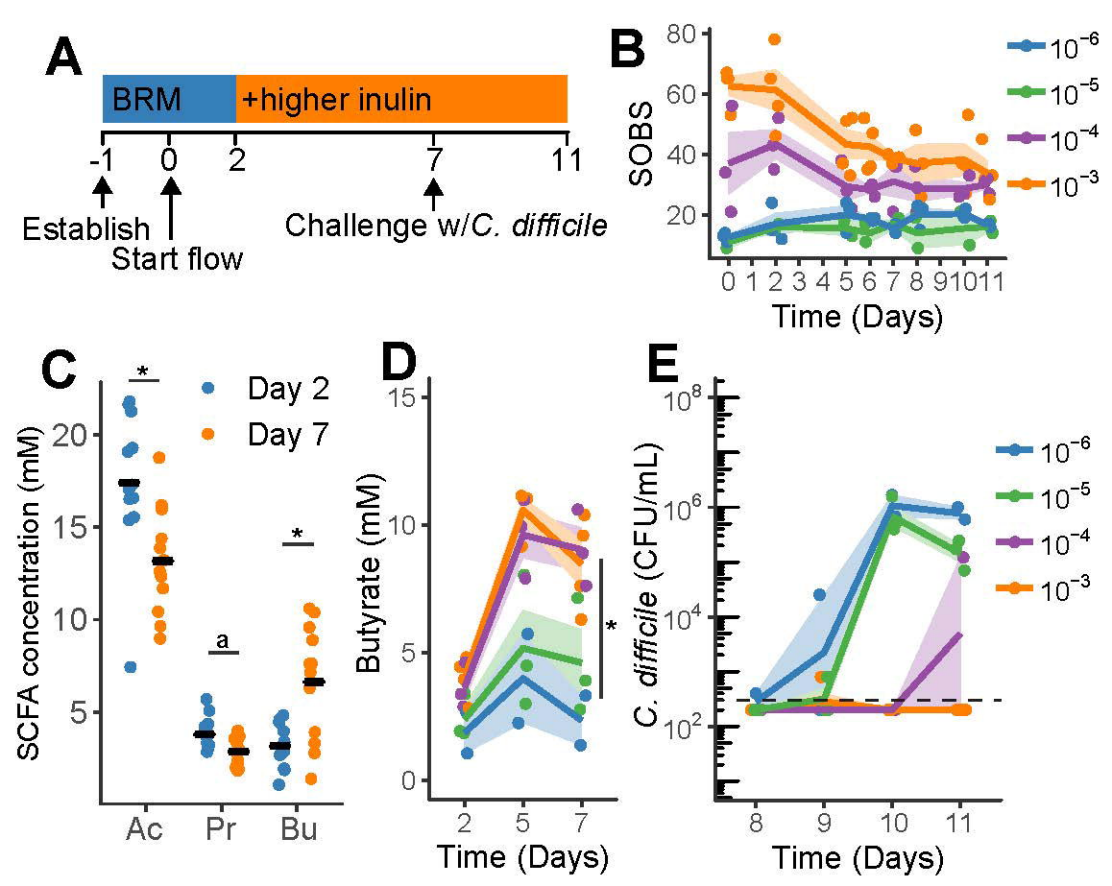
A
BRM
+higher inulin
-1
0
2
7
11
Establish
Start flow
Challenge w/C. difficile
B
SOBS
80
60
40
20
0 1 2 3 4 5 6 7 8 9 10 11
Time (Days)
10^-6
10^-5
10^-4
10^-3
C
SCFA concentration (mM)
20
15
10
5
Day 2
Day 7
*
a
*
Ac
Pr
Bu
D
Butyrate (mM)
15
10
5
0
*
2
5
7
Time (Days)
E
C. difficile (CFU/mL)
10^8
10^6
10^4
10^2
8
9
10
11
Time (Days)
10^-6
10^-5
10^-4
10^-3